Calorimetric and electrical transport properties of stoichiometric $La_{1-x}Sr_xMnO_3$ compounds

2003 J. Phys.: Condens. Matter 15 7763

(http://iopscience.iop.org/0953-8984/15/45/015)

INSTITUTE OF PHYSICS PUBLISHING JOURNAL OF PHYSICS: CONDENSED MATTER

J. Phys.: Condens. Matter **15** (2003) 7763–7776 PII: S0953-8984(03)62256-3

Calorimetric and electrical transport properties of stoichiometric $La_{1-x}Sr_xMnO_3$ compounds

A Michalopoulou[1], E Syskakis[2] and C Papastaikoudis[1]

[1] Institute of Materials Science, National Centre of Scientific Research 'Demokritos', GR-153 10 Ag Paraskevi, Athens, Greece
[2] Section of Solid State Physics, University of Athens, Gr-157 84 Zografou, Athens, Greece

Received 15 April 2003, in final form 22 September 2003
Published 30 October 2003
Online at stacks.iop.org/JPhysCM/15/7763

Abstract

Heat capacity and electrical resistivity investigations are carried out for stoichiometric $La_{1-x}Sr_xMnO_3$ manganite compounds. The temperature of the peak of the heat capacity c_p associated with ferromagnetic transition is in agreement with the resistivity measurements. The electrical resistivity shows a roughly AT^2 dependence over a wide temperature range, where the coefficient A decreases as the content of Sr increases. The results show that the Kadowaki–Woods empirical relation is not valid. It is attempted to explain the dependence of A on the x content of Sr within the framework of electron–electron Umklapp scattering.

1. Introduction

Lanthanum manganese oxides have been studied intensively in recent years because these compounds show a great variety of magnetic and transport properties.

The parent compound $LaMnO_3$, doped with divalent Sr^{2+} ions, shows a ferromagnetic metallic state below a Curie temperature T_C and above the critical concentration $x \geqslant 0.17$ [1–3]. The partial substitution of trivalent La^{3+} by the divalent Sr^{2+} ions in the antiferromagnetic parent insulator $LaMnO_3$ leads to the presence of a mixed valence of Mn^{3+} and Mn^{4+} ions with the electron configurations $(t_{2g})^3(e_g)^1$ and $(t_{2g})^3(e_g)^0$ respectively. The e_g electrons (holes) can then hop between Mn^{3+} and Mn^{4+} ions via a 'double exchange' interaction mechanism [4–7]. The transfer of the extra e_g electron between the neighbouring Mn ions is carried out through the O^{2-} ions. Among the four $3d^4$ electrons on the Mn site, the strong Hund coupled $(t_{2g})^3$ electrons may be viewed as a single local spin ($S = 3/2$), since the t_{2g} electrons show smaller hybridization than e_g states with oxygen 2p states. However, the deviation of the e_g band filling ($n = 1 - x$) from integer value ($n = 1$), or the so-called hole doping, produces a barely metallic and ferromagnetic ground state in $La_{1-x}Sr_xMnO_3$ for $x \geqslant 0.17$. The distinct feature of such a state in manganese oxides is that there exists a strong exchange interaction between the itinerant e_g electrons (holes) and the localized t_{2g} spins.

The current intense interest in $La_{1-x}Sr_xMnO_3$ manganites is focused mainly on the magnetic and the transport properties [2, 3], but there have been a limited number of studies carried out on the heat capacity [8–12]. Woodfield *et al* [9] have measured the heat capacity of the $La_{1-x}Sr_xMnO_3$ system as a function of the Sr concentration ($x = 0.00$–0.30) between 0.5 K and 10 K, where they have studied the nature of the transition. Okuda *et al* [10] have measured the heat capacity of $La_{1-x}Sr_xMnO_3$ ($0.12 < x < 0.40$) single crystals in the temperature range between 3 K and 10 K. They have found that the electronic heat capacity coefficient, $\gamma = 3$–5 mJ mol^{-1} K^{-2}, indicates minimal mass-renormalization even near the metal–insulator transition. Uhlenbruck *et al* [11] have measured the heat capacity of the $La_{0.875}Sr_{0.125}MnO_3$ single crystals from 20 K to 290 K in magnetic fields up to 14 T in order to study the influence of the magnetic field on the different phase transitions. Recently Liu *et al* [12] have reported an extended investigation on transport, magnetic and heat capacity properties, on a series of melt-grown crystal $La_{1-x}Sr_xMnO_3$ which confirm the complex evolution of phases in the range $0.08 < x < 0.19$. Thus, motivated by the lack of detailed measurements in $La_{1-x}Sr_xMnO_3$ manganites that characterize the heat capacity anomaly at the ferromagnetic ordering temperature, we have carried out a systematic heat capacity study simultaneously with the resistivity as a function of the Sr content. However, the electrical transport mechanism of the manganites especially in the ferromagnetic metallic phase below T_C is poorly understood. The main goal of this work is to examine—with the aid of the heat capacity—how the metallic ferromagnetic phase develops with Sr doping from the parent compound $LaMnO_3$ and to study the mechanism responsible for the Sr content x dependence of the coefficient A in the T^2 law.

2. Experimental procedure

Polycrystalline $LaMnO_3$ and $La_{1-x}Sr_xMnO_3$ samples were prepared using the hot petroleum extraction technique [13]. According to this technique the perovskite powders have been prepared using nitrate salt ($La(NO_3)_36H_2O$, $Sr(NO_3)_2$, and $Mn(NO_3)_24H_2O$ of a purity of 99.9%) solutions which were converted at 160–180 °C into fine powdered salt mixtures of high homogeneity. The dried salt mixtures were washed thoroughly before calcinations with CCl_4 in order to reduce residual adhered hydrocarbons. A complete characterization of the dried products by XRD and SEM techniques has been undertaken all the way through calcinations. The formation of perovskite phase during calcinations in air occurred at above 500 °C and was completed at 900 °C. The powders consisted of spherical grains with an average diameter of 5 μm. The cation and the impurity content of the powders after the calcinations have been determined by inductively coupled plasma-photoemission spectroscopy (ICP-PES). The observed deviations from the intended composition were within the precision of the ICP-PES results. The major impurity of the powders was carbon with $\leqslant \pm 0.5\%$. For the transport measurements the $LaMnO_3$ and $La_{1-x}Sr_xMnO_3$ powders were cold pressed into rectangular bars and then sintered in air at 1400 °C for 24 h. The crystal structure of the manganite samples was characterized using a Siemens D 500 x-ray powder diffractometer. The XRD investigations have shown that the specimens were single-phase perovskites with either orthorhombic or hexagonal symmetry depending on the concentration. The lattice parameters a, b, c, the unit cell volume V_c and the crystallographic symmetry of the investigated compounds are listed in table 1. From table 1 one can seen that the unit cell volume decreases nearly linearly with increasing Sr content. The bars have masses of about 1.5 g with nominal Sr concentrations of 0.00, 0.10, 0.14, 0.16, 0.20, 0.30 and 0.40. The heat capacity measurements were carried out using a sensitive home-made heat pulse adiabatic calorimeter for the low temperature region (5–300 K), and a Du Pont R 90 differential scanning calorimeter for high temperatures

Table 1. Lattice parameters (a, b, c), unit cell volume (V_c) and crystallographic symmetry of $LaMnO_3$ and $La_{1-x}Sr_xMnO_3$ compounds.

Compound	a (Å)	b (Å)	c (Å)	V_c (Å^3)	
$LaMnO_3$	5.5430	5.6360	7.7560	60.575	Orthorhombic
$La_{0.90}Sr_{0.10}MnO_3$	5.5160	5.5340	7.7960	59.455	Orthorhombic
$La_{0.86}Sr_{0.14}MnO_3$	5.5030	5.5470	7.7750	59.329	Orthorhombic
$La_{0.84}Sr_{0.16}MnO_3$	5.5400	5.5400	13.371	59.272	Hexagonal
$La_{0.80}Sr_{0.20}MnO_3$	5.5310	5.5310	13.370	59.042	Hexagonal
$La_{0.70}Sr_{0.30}MnO_3$	5.5099	5.5099	13.369	58.581	Hexagonal
$La_{0.40}Sr_{0.60}MnO_3$	5.4877	5.4877	13.361	58.077	Hexagonal

(220–400 K). The low temperature calorimeter was calibrated by measuring the heat capacity of a high purity (6N) copper specimen. The samples were attached to the thermal isolated calorimeter platform (Al_2O_3) using a small amount of Apiezon-N grease of known heat capacity to ensure good thermal contact. A calibrated carbon resistance and a Pt thin film located on the calorimeter platform were used as secondary thermometer, while as primary thermometer a calibrated GaAlAs diode, a germanium and a platinum resistances were used. A mechanical switch proved thermal contact between the tray and isothermal shield. No exchange gas was used to cool the sample. The heat capacity was measured with an accuracy better than 4% as checked against the copper calibration sample. The heat capacity of the $LaMnO_3$ and $La_{0.80}Sr_{0.20}MnO_3$ compounds were measured also at temperatures down to 4.2 K in order to determine the density of states. The electrical resistivity of the specimens was studied using a standard four-point dc measurements set-up.

3. Results and discussion

3.1. Heat capacity

The heat capacity of the present investigated $La_{1-x}Sr_xMnO_3$ manganite perovskites are shown in figure 1, with c_p plotted versus T. The heat capacity shows an anomaly which is characterized by a peak at a certain temperature T_p. This temperature shifts to high values with increase of the Sr content. Figure 2 shows the peak temperature T_p as a function of Sr concentration x, with the Néel (T_N) and Curie (T_C) temperatures taken for the same manganites from previous magnetization measurements [2, 3]. The figure shows that T_p is very close to the critical temperatures T_N and T_C and goes through a maximum between $x = 0.30$ and 0.40. As results from the agreement between T_p, T_N and T_C, one can conclude that the above mentioned anomaly in heat capacity c_p is due to a magnetic phase transition. One can identify that the c_p measurements show the same magnetic phase diagram that has been extracted from the magnetization [3]. According to Urushibara *et al* [3] and Tokura *et al* [2] the Jahn–Teller disordered parent compound $LaMnO_3$ undergoes the phase transition to the spin-canted antiferromagnetic insulator below $x = 0.10$. With further doping of the $LaMnO_3$ system with Sr, the ferromagnetic metallic phase appears below the Curie temperature T_C that abruptly increases with concentration up to 0.35. In the narrowly doped range $0.10 \leqslant x \leqslant 0.17$ a ferromagnetic insulating phase is present, in which the double-exchange carrier is subject to Anderson localization but can still mediate from ferromagnetic interaction between neighbouring states and realize the ferromagnetic state in a bound-percolation manner. At high temperatures there appears to occur a transition from the paramagnetic insulator to the

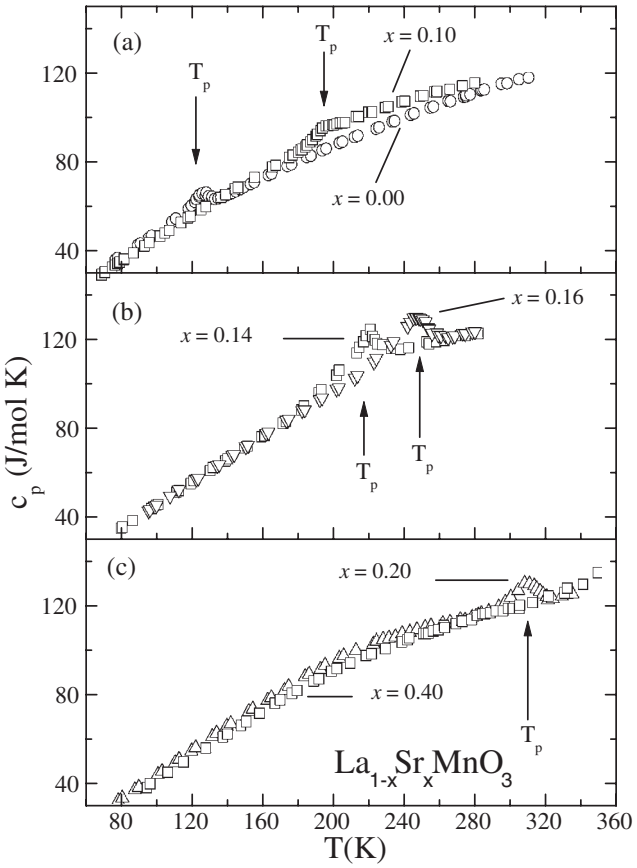

Figure 1. The heat capacity c_p as a function of the temperature T for $La_{1-x}Sr_xMnO_3$ compounds.

paramagnetic metal around the concentration $x = 0.30$. By measuring the heat capacity of a $La_{0.875}Sr_{0.125}MnO_3$ single crystal in magnetic fields up to 14 T, Uhlenbruck *et al* [11] have found, in contradiction to the present results, two other intense structural transitions besides for a ferromagnetic transition. The high temperature peak (∼270 K) is attributed to a structural phase transition from an orthorhombic to a cooperative Jahn–Teller disordered phase [14]. The low temperature peak (∼150 K) is caused by a transition accompanied by a change in structure [14, 15] and by charge ordering [15–21]. On the other hand, the anomaly in the heat capacity at ∼187 K, which is due to the paramagnetic–ferromagnetic transition, is not pronounced as in the present results. The differences between the present measurements and those of Uhlenbruck *et al* [11] can be attributed to the fact that have used single crystalline samples. Recent heat capacity measurements on single crystals of $La_{1-x}Sr_xMnO_3$ [12] have shown that in the compositional range $0.08 < x < 0.19$ the phase diagram is more complicated. The ferromagnetic transition is strongly coupled to a structural phase transition from a Jahn–Teller distorted O′ phase to a pseudocubic O″ orthorhombic phase.

Figure 3 shows the heat capacity in the form c_p/T versus T^2 in the low temperature range between 5 and 11 K for the parent $LaMnO_{3+\delta}$ and $La_{0.80}Sr_{0.20}MnO_3$ compounds. The linearity of the curves above 5 K indicates that the data fit the expression

$$c_p/T = \gamma + \beta T^2. \tag{1}$$

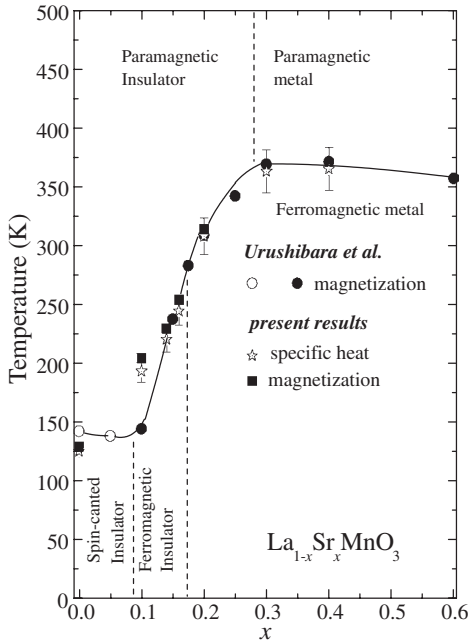

Figure 2. The temperature T_p corresponding to the peak of the c_p as a function of the Sr content x.

Neither upturn nor downturn behaviour for the c_p/T versus T^2 plot is observed down to 5 K, which indicates the absence of a spin-wave contribution and enables us to determine the γ values unambiguously. For comparison, previous measurements on $LaMnO_{3+\delta}$ ($\delta = 0.11$) [22] polycrystalline and $La_{0.80}Sr_{0.20}MnO_3$ [10] single crystalline compounds are also displayed. The deviation of the present results from these of Ghivelder *et al* [22] on $LaMnO_{3+\delta}$ can be attributed to the different oxygen compositions. The values of the linear coefficient γ turn out to be 0.65 ± 0.20 mJ mol^{-1} K^{-2} for the parent $LaMnO_{3+\delta}$ compound and 1.60 ± 0.20 mJ mol^{-1} K^{-2} for the Sr doped sample. The present γ value of the parent $LaMnO_3$ compound is in good agreement with the γ values of the compounds in the spin-canted antiferromagnetic insulating phase [22], while the γ value of the ferromagnetic metallic $La_{0.80}Sr_{0.20}MnO_3$ compound is about a factor 2.5 smaller than that of previous measurements for the same Sr content [10]. For the coefficient β of the lattice contribution we obtain 0.340 ± 0.004 mJ mol^{-1} K^{-4} for $LaMnO_3$ and 0.150 ± 0.004 mJ mol^{-1} K^{-4} for $La_{0.80}Sr_{0.20}MnO_3$. The corresponding Debye temperature $\Theta_D = [(5 \times 1944)/\beta]^{1/3}$ is 306 K and 402 K for $LaMnO_3$ and $La_{0.80}Sr_{0.20}MnO_3$ respectively. The present value of the Debye temperature of the $La_{0.80}Sr_{0.20}MnO_3$ compound is in very good agreement with early measurements on $La_{0.80}Sr_{0.20}MnO_3$ [10]. If one assumes that the linear term γ in the heat capacity arises entirely from the presence of charge carriers, which in the free-electron model of a metal is given by $\gamma = \pi^2 k_B^2 N(\varepsilon_F)/3$, one can calculate the density of states $N(\varepsilon_F)$ at Fermi energy. The above mentioned values of the linear coefficient γ for the parent $LaMnO_3$ and $La_{0.80}Sr_{0.20}MnO_3$ compounds yields $N(\varepsilon_F) = 0.21 \times 10^{24}$ eV^{-1} mol^{-1} and 0.66×10^{24} eV^{-1} mol^{-1}, respectively. Assuming further that all holes introduced by the dopant are mobile carriers then the free-electron value of γ can be calculated. With a molar volume V of 36 cm^3 [23] and with the doping concentration x we find a charge density of $n(x) = 1.7 \times 10^{22} x$ carriers cm^{-3}. The free-electron value of γ for concentration $x = 0.2$

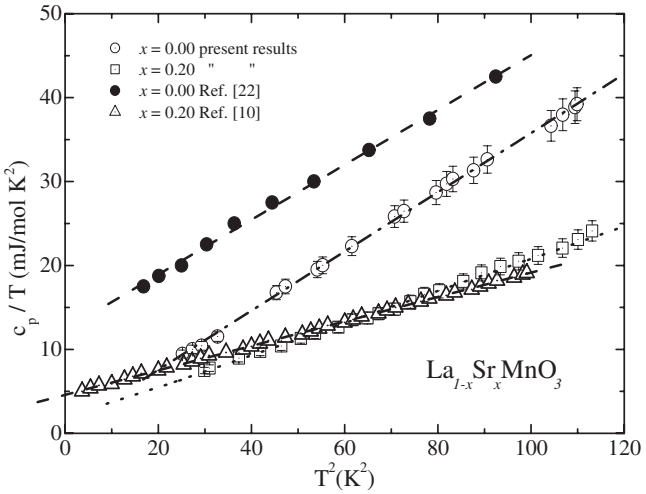

Figure 3. c_p/T versus T^2 for the parent $LaMnO_3$ and the $La_{0.80}Sr_{0.20}MnO_3$ compound.

is $\gamma_{free} = 0.87$ mJ mol^{-1} K^{-2}. Thus the thermal effective mass $m_{thermal} = (\gamma_{obs}/\gamma_{free})\, m_o$ is about $2m_o$, where m_o is the bare mass. This mass enhancement arises mainly from many body effects such as the electron–electron correlation, and the electron–phonon interaction.

Another feature of this figure is that the phonon contribution to the heat capacity of the insulating $LaMnO_3$ compound is clearly higher than that for the sample in the ferromagnetic metallic state. This is probably due to the different phonon density of states between $LaMnO_3$ and $La_{0.80}Sr_{0.20}MnO_3$ compounds, which results from the change in the crystal structure, from cubic to orthorhombic, during the Sr doping.

In order to estimate the entropy ΔS_{magn} associated with the magnetic transition in each compound a smooth background has been subtracted from the experimental data of heat capacity c_p as a lattice contribution. This procedure is only a rough approximation of the real lattice contribution to the heat capacity. A second estimation method of the change of the magnetic entropy ΔS_{magn} is the following. It is known that the parent compound $LaMnO_3$ for temperatures $T \geqslant 120$ K is in the paramagnetic phase. In this temperature region the heat capacity can be attributed entirely to lattice contribution. We assume moreover that the lattice contribution to the heat capacity of $LaMnO_3$ is not expected to change significantly during the partial replacement of La with Sr. With subtraction of the lattice contribution of the $LaMnO_3$ sample from the experimentally determined heat capacity of $La_{1-x}Sr_xMnO_3$ compounds and by integrating the area below the peak, one can obtain the magnetic entropy for each sample. Figure 4 shows the entropy ΔS_{magn} as a function of the Sr content x for both methods of estimation. ΔS_{magn}, obtained for parent compound $LaMnO_3$, approaches the value of 1 J mol^{-1} K^{-1}. With increase of Sr content, ΔS_{magn} increases, goes through a maximum at about $x = 0.13$, then decreases and for $0.20 \leqslant x \leqslant 0.40$ approaches the values of 0.7 J mol^{-1} K^{-1} and 5.8 J mol^{-1} K^{-1} respectively. The values of ΔS_{magn} estimated with the first method (solid circles) have been reported previously [24]. In the same figure are also plotted the ΔS_{magn} data taken from the recent work of Liu *et al* [12] on $La_{1-x}Sr_xMnO_3$ single crystals. One can see that there is a similarity between these two independent measurements. The results of Liu *et al* [12] are in good agreement with the present results estimated with the first method. The only difference is the present half-value of ΔS_{magn} for $x = 0.00$. The entropy values of both measurements are smaller than the

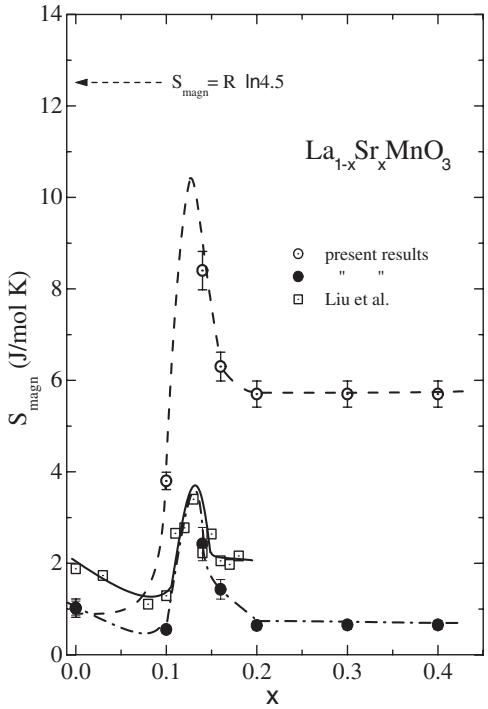

Figure 4. The entropy change ΔS_{magn} as a function of the Sr content x. The lines are guides to the eye.

estimated value $\Delta S_{\text{est}} = R\ln(2S+1) = 12.5$ J mol^{-1} K^{-1} expected from an $S = 1.75$ spin system. Low values of the entropy have been reported earlier also by Ramirez *et al* [25] for $La_{1-x}Ca_xMnO_3$ and by Lees *et al* [26] for $Pr_{0.6}(Ca_{1-x}Sr_x)_{0.4}MnO_3$ perovskites. In order to see if the maximum value of ΔS_{magn} is caused by a magnetic transition or other effects, the heat capacity for the samples with 0.00, 0.10, 0.14, 0.16 and 0.20 Sr has been measured, both during the heating and cooling process. The results are displayed in figure 5. It is obvious that only the compound $La_{0.86}Sr_{0.14}MnO_3$ exhibits a definite hysteresis. This means that in the range $0.10 \leqslant x \leqslant 0.16$ the compounds undergo a first order transition besides the second order ferromagnetic transition, which contributes to the total change of the entropy ΔS. The most probable cause can be a crystallographic transition from Jahn–Teller distorted O′ phase into a pseudocubic O″ phase [27]. Liu *et al* [12] believe also that the appearance of the maximum of ΔS_{magn} between 0.12 and 0.15 Sr is due to the orbital disorder–order and disorder–order transitions at T_{00} and critical temperature T_C.

3.2. Electrical resistivity

Figure 6 shows the temperature dependence of the resistivity $\rho(T)$ as a function of Sr content. The arrows in the ρ–T curves indicate the Curie temperature T_C, which was determined from the magnetization curves M–T [3]. The resistivity of the parent $LaMnO_3$ compound increases exponentially with decreasing temperature and no ferromagnetic transition is observed. This means that $LaMnO_3$ manganite is in the insulating state, where the resistivity showed activated transport properties obeying the low $\rho = \rho_o \exp(-E_a/k_BT)$. A fitting procedure to the

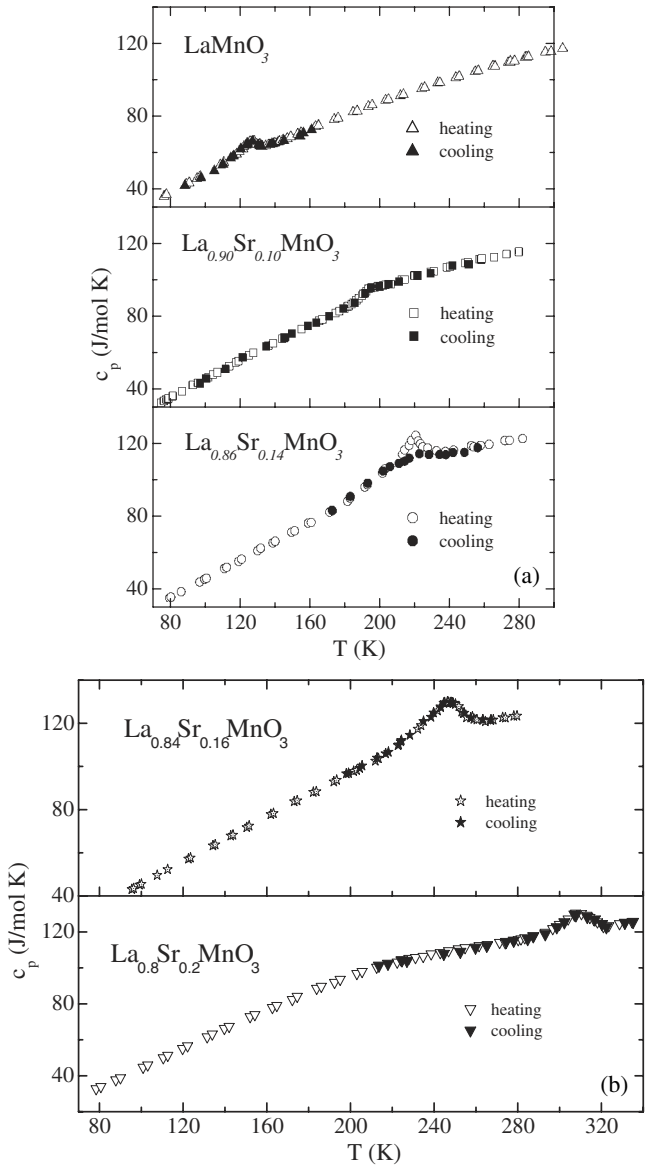

Figure 5. The heat capacity c_p as a function of T for the compounds with 0.00, 0.10, 0.14, 0.16 and 0.20 Sr during both the heating and cooling process.

experimental data gives an activation energy $E_a \cong 170$ meV, which is close to previous results [28]. The resistivities $\rho(T)$ for $x \neq 0.00$ show a change at certain temperatures which are not so outstanding as in previously reported results of Urushibara *et al* [3]. Particularly, $\rho(T)$ at $x = 0.10$, 0.14 and 0.16 Sr decreases as the temperature increases until the characteristic temperatures $T_{CO} \sim 190$, 204 and 145 K, then is temperature independent (plateau) and shows a weak break at 209, 243 and 260 K respectively, which correspond to the Curie temperatures T_C. Finally in the high temperature paramagnetic phase the resistivity continues to decrease as T increases. This means that the ρ–T curves behave like a non-metal,

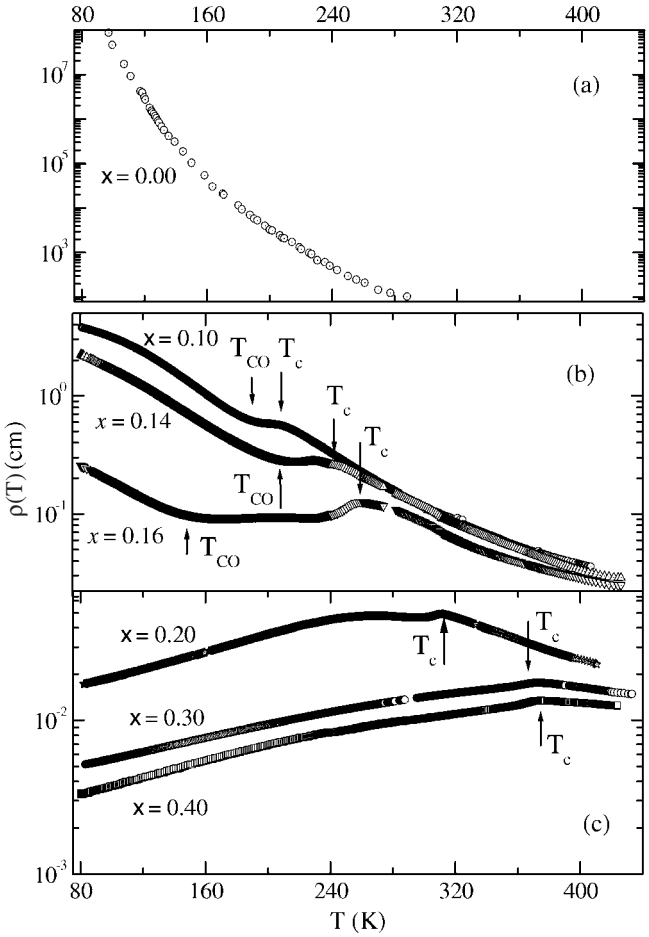

Figure 6. $\rho(T)$ as a function of T for different Sr content x.

i.e. $\mathrm{d}\rho/\mathrm{d}T < 0$. The transition temperatures T_{CO} at 190, 204 and 145 K can be attributed to the charge ordering [29]. The shape of the ρ–T curves for $x \geqslant 0.20$ Sr changes. For temperatures below 350 K, the resistivity $\rho(T)$ increases with increasing temperature. This means that for $T \leqslant 350$ K the samples behave like a metal. In order to see the temperature dependence of the resistivity in more detail, in figures 7 and 8 we have illustrated the quantities $[\rho(T) - \rho(4.2\ \mathrm{K})]/T$ as a function of T in a log–log plot for the compounds in the metallic phase ($x = 0.20$, 0.30 and 0.40 Sr), where $\rho(4.2\ \mathrm{K})$ is the resistivity at 4.2 K. From these figures it can be seen that the behaviour of resistivities of these compounds is complicated and their temperature dependence cannot be characterized by a single power law. Figure 7 shows that $\rho(T) - \rho(4.2\ \mathrm{K})$ of the compound with $x = 0.20$ Sr between 80 and 240 K is proportional to $T^{1.97}$. From figure 8 it can be seen that $\rho(T) - \rho(4.2\ \mathrm{K})$ of the compounds with $x = 0.30$ and 0.40 Sr has nearly the same temperature dependence. For the compound with $x = 0.30$, $\rho(T) - \rho(4.2\ \mathrm{K})$ varies approximately as $T^{2.17}$ in the temperature range 80–135 K, then as $T^{1.80}$ between 135 K and 265 K, and finally as $T^{1.30}$, while for the compound with $x = 0.40$, $\rho(T) - \rho(4.2\ \mathrm{K})$ varies as $T^{2.00}$ between 80 K and 145 K, then as $T^{1.80}$ between 145 K and 225 K and finally as $T^{1.30}$. The dashed lines in these figures correspond to the

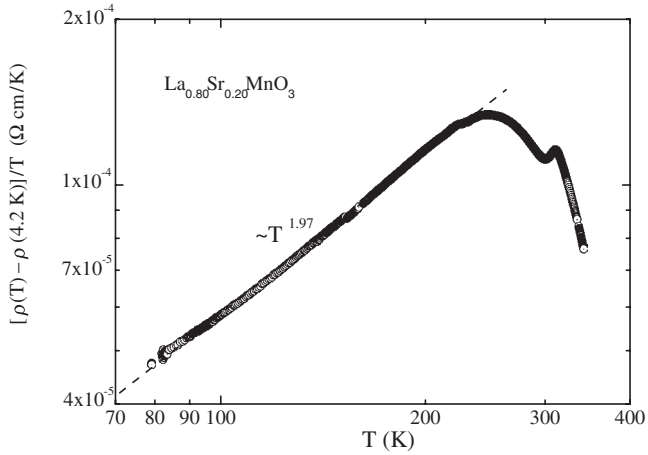

Figure 7. The quantity $[\rho(T) - \rho(4.2\ \mathrm{K})]/T$ as a function of T for the $La_{0.80}Sr_{0.20}MnO_3$.

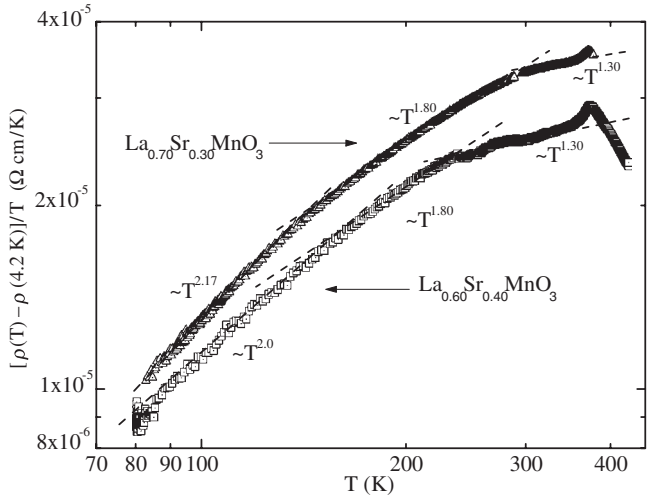

Figure 8. The quantity $[\rho(T) - \rho(4.2\ \mathrm{K})]/T$ as a function of T for the $La_{0.70}Sr_{0.30}MnO_3$ and $La_{0.60}Sr_{0.40}MnO_3$.

linear fits. It is apparent that the resistivity in the ferromagnetic metallic phase is characterized roughly by the relation $\rho(T) \sim \rho_o + AT^2$, over a wide temperature range (at least up to 250 K). At first sight it seems to show a conventional Fermi liquid behaviour. Notably, such a quadratic temperature law has been also reported in the same manganite system previously by Urushibara *et al* [3]. They have attributed the T^2 dependence to the normal electron–electron scattering (NEES) proposed by Landau, Pomeranchuk and Barber [30]. In table 2 are listed the $\rho(4.2\ \mathrm{K})$, the coefficient A and the ratio of A/γ^2, where γ is the low temperature specific heat coefficient. Looking at table 2 one can may notice that

(i) the T^2 coefficient A of the present manganites appears to be remarkably enhanced with decreases of Sr content x, and
(ii) the ratio A/γ^2 is too large to fit the empirical Rice–Kadowaki–Woods law [31, 32], which is characteristic for the transition metals and strongly electron correlated systems.

Table 2. The electrical resistivity at 4.2 K, the T^2 coefficient A and the Kadowaki–Woods ratio A/γ^2 of the $La_{1-x}Sr_xMnO_3$ system of various Sr content x.

x	ρ_0 (mΩ cm)	A ($\mu\Omega$ cm K^{-2})	A/γ^2 ($\mu\Omega$ cm mol^2 K^2 mJ^{-2})
0.20	13.6	0.57	0.27
0.30	4.3	0.13	0.08
0.40	2.6	0.11	0.05

In the transition metals A/γ^2 takes the 'universal' value of 0.9×10^{-6} $\mu\Omega$ cm mol^2 K^2 mJ^{-2} [31], while in the strongly correlated electron systems (heavy fermion (HF) systems) the value 1.0×10^{-5} $\mu\Omega$ cm mol^2 K^2 mJ^{-2} [32]. One exception is for the α-Mn metal where A and A/γ^2 take the values $\sim$0.15 $\mu\Omega$ cm K^{-2} and $\sim 6 \times 10^{-4}$ $\mu\Omega$ cm mol^2 K^2 mJ^{-2} respectively [33]. The present high A/γ^2 values, which are about three to four orders of magnitude larger than the empirical 'universal' value for the strongly electron systems, may signal that the underlying scattering mechanism corresponding for T^2 dependence of the resistivity is not necessarily only the electron–electron scattering process. It seems to be related to an extra scattering process of carriers. On the other hand a $\rho(T) \sim AT^2$ dependence can be also of magnetic origin. Such temperature dependence is observed in the conventional ferromagnetic metals Ni, Co and Fe at low temperatures. The values of the coefficient A of these metals lie between 1.3×10^{-5} $\mu\Omega$ cm K^{-2} and 1.6×10^{-5} $\mu\Omega$ cm K^{-2} [33], which are about four orders of magnitude smaller than the values of the present half-metallic ferromagnetic manganites. In conventional itinerant weak ferromagnetic metals, where both spin channels conduct currents, the T^2 dependence of the resistivity is attributed to absorption and emission of a single magnon (one-magnon–electron process) [34, 35]. On the other hand, for a truly half-metallic ferromagnet like the present compounds, the conduction electrons are perfectly spin-polarized and the Fermi energy is absent in the minority-spin band. Kubo and Ohata [7], based on such a rigid-band picture, have shown that while the one-magnon–electron scattering process is exponentially suppressed by a factor $\exp(-\varepsilon_g/k_BT)$, where ε_g is the minority-spin band gap at Fermi energy, the two-magnon–electron scattering process can lead to a $T^{9/2}$ temperature dependence. Wang and Zhang [36] calculated the resistivity of a nearly half-metal ferromagnet system where the minority-spin channel has a finite density of states at the Fermi level but does not conduct current because of the Anderson localization. In this case, spin-flip scattering involving only single magnons can occur with a finite probability. They derived a resistivity $\rho \propto T^{2.5}$ at high temperatures (above 60 K), which crosses over to $\rho \propto T^{1.5}$ at low temperatures.

Recently Furukawa [37] has taken into account the spin fluctuations at finite temperatures, which break down the perfect spin polarization of the conduction electrons and modify the electronic band structure. The result of this depolarization is the creation of a minority-spin band, which has common Fermi energy with the majority-spin band. Once the thermally activated minority band is created and occupied, then a one-magnon scattering is allowed. This anomalous one-magnon scattering process gives to the resistivity a $\propto T^3$ dependence. Experimentally, it has been reported that the low temperature ($T < 40$ K) resistivity for non-stoichiometric $La_{0.95-x}Sr_xMnO_3$ system scales as $\propto T^3$ [38]. With temperature increases, the magnitude of the minority-spin band also increases, and in the paramagnetic state ($T > T_C$) its occupation is equal to that of the majority-spin band. At temperatures $T > 50$ K the thermal fluctuation of spins begins to destroy the half-metallic state of the manganite system and probably the conventional one-magnon scattering process should also play an important role, which can lead to a $\propto T^2$ dependence [39]. Very recently Calderón and Brey [40],

by studying low energy and low temperature electronic properties of double-exchange systems, have found that the low energy spin excitations are a linear combination of ion and electron spin waves. They have shown that static disorder in the hopping amplitude couples with the spin fluctuations and creates a resistivity, which, in contradiction to the Furukawa model increases with temperature as $\propto T^{3/2}$ and $\propto T^3$. They maintain the opinion that the $T^{3/2}$ term is more important than the T^3 term up to temperatures higher than the critical one and also that the magnitude of this resistivity is in agreement with experimental data. According to what has been mentioned above, the electron–electron scattering and the single electron–magnon scattering process cannot individually explain the anomalous large T^2 coefficient A and its x dependence, unless certainly one assumes that the electron–magnon scattering process contributes to the resistivity in addition to the electron–electron scattering.

On the other hand Maebashi and Fukuyama [41] have studied on the basis of the Fermi liquid theory the electrical resistivity due only to mutual Coulomb interaction of the d-dimensional lattice electron system in the presence of Umklapp scattering processes. They have shown in a Hubbard model that normal scattering processes generally contribute to the resistivity, if electron–electron Umklapp scattering processes are present. In the case of $d = 2$, Maebashi and Fukuyama [41] have shown that the resistivity is proportional to AT^2. In the special case of the square lattice, the Fermi liquid coefficient A of the T^2 term in the second order of the interaction is given by

$$A \propto (3/32)(U^2/e^2t^4)(t/\mu_o), \tag{2}$$

where U is the on-site Coulomb interaction, t the transfer integrals and μ_o the chemical potential of the non-interacting system. In the 2D Hubbard model and for transfer integrals that are only between the nearest neighbours, the Fermi surface (FS) becomes a square and touches the Brillouin zone (BZ) at the same time at half-filling. As the system approaches half-filling ($\mu_o \to 0$), the coefficient A diverges. This feature is due to the flatness of the FS, which results if the Umklapp processes become very effective. The doping rate x is related to the chemical potential μ_o by $x \propto (|\mu_o|/t)\log(|\mu_o|/t)$ near the half-filling where the logarithmic factor reflects the van Hove singularity. Therefore, the coefficient A diverges as $(1/x)\log(1/x)$ when the doping x approaches zero. This means that the coefficient A decreases as the doping rate x increases, because the fraction of Umklapp scattering processes decreases. If one includes the transfer integrals t' between next nearest neighbours as well, the FS touches the BZ at some filling other than half. The Fermi line is not more composed of straight lines, as the sides of a square, but it is composed of curves. In the t–t' Hubbard model, the Umklapp scattering is very intensive and enhances the coefficient A near the van Hove point, where the FS touches the BZ, but is less or not singular than for the case $t' = 0$ near the half-filling [43]. Figure 9 shows the calculated dependence of the coefficient A on doping x in a log–log plot together with the present experimental results and those of Urushibara *et al* [3] and Okuda *et al* [42]. The figure contains also for comparison the coefficient A of the HF system $CeRu_2Si_2$ as a function of hydrostatic pressure [44]. The most surprising result is a similarity between the theoretical and experimental data both in the manganites and in the heavy fermion system. This is probably an indication that the Umklapp electron–electron scattering processes are responsible for the high values of the coefficient A and their dependence on the doping of Sr or on the pressure in the case of HF systems. The difference in the magnitude of the coefficient A between the present results of polycrystalline samples and these of single crystals can be attributed to the sample structure. It is possible that in the present samples in addition to the electron–electron scattering, also a scattering of the electrons on the grain boundaries takes place. On the other hand the coefficient A of the e-type HF $CeRu_2Si_2$ system is strongly affected by the application of hydrostatic pressure and therefore as the pressure increases the

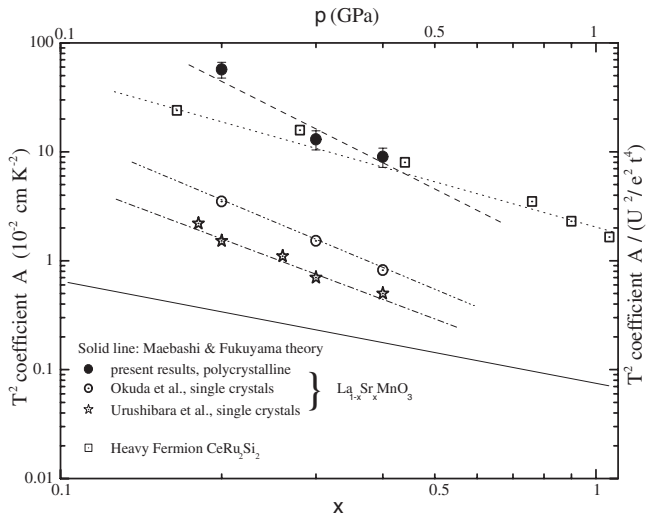

Figure 9. The dependence of the T^2 coefficient A on the Sr content x and the static pressure p of the manganites and of the HF $CeRu_2Si_2$ system respectively.

A coefficient decreases and expands the temperature region in which the quadratic law appears. According to the above,one can assume that the hydrostatic pressure reduces the volume of the unit cell of crystal lattice of the HF system, which translates into a growth of the unit cell in reciprocal lattice space. This has the result that the BZ moves away from the FS and consequently the fraction of Umklapp scattering processes is reduced. In this rough model it is assumed that the FS is not influenced from the pressure. In the same sense we try to explain physically the present Sr content dependence of the coefficient A of the manganites. As was mentioned in the introduction, by the substitution of the La^{3+} ions (radius of 0.136 nm) with the divalent Sr ions (0.144 nm) a part of the Mn^{3+} ions (0.0645 nm) are replaced with the Mn^{4+} ions (0.053 nm) [28]. This means that the unit cell of the crystal lattice is reduced similarly to the application of external hydrostatic pressure. This internal chemical pressure, which increases as the content of the Sr ions increases, results in the growth of the unit cell in reciprocal lattice space. According to the above the BZ moves away from the FS and consequently the Umklapp scattering processes are reduced.

4. Conclusions

We have measured the low temperature specific heat and the electrical resistivity between 77 K and 300 K of the stoichiometric $La_{1-x}Sr_xMnO_3$ compounds. The calorimetric measurements have shown that the temperature T_p corresponding to the peak of the specific heat follows the same Sr content dependence as the Néel T_N and Curie T_C temperature extracted from the magnetization measurements. The magnetic entropy change ΔS_{magn} shows a maximum in the range $0.10 \leqslant x \leqslant 0.16$ and is probably due to a first order crystallographic transition from the Jahn–Teller distorted O′ phase into a pseudocubic O″ phase. The resistivity measurements of the compounds in the ferromagnetic metallic phase show that the T^2 coefficient A exhibits high values, a Sr content dependence and does not obey the Kadowaki–Woods empirical law. The cause of this behaviour is due to the participation of the Umklapp process in the electron–electron scattering.

Acknowledgments

CP gratefully acknowledges Hideaki Maebashi for numerous discussions and the Empeirikion Foundation for financial support.

References

[1] Jonker G H and Van Santen J H 1950 *Physica* **16** 337
Jonker G H 1956 *Physica* **22** 707
[2] Tokura Y, Urushibara A, Moritomo Y, Arima T, Asamitsu A, Kido G and Furukawa N 1994 *J. Phys. Soc. Japan* **63** 3931
[3] Urushibara A, Moritomo Y, Arima T, Asamitsu A, Kido G and Tokura Y 1995 *Phys. Rev.* B **51** 14103
[4] Zener C 1951 *Phys. Rev.* **82** 403
[5] Anderson P W and Hasegawa H 1955 *Phys. Rev.* **100** 675
[6] de Gennes P-G 1960 *Phys. Rev.* **118** 141
[7] Kubo K and Ohata N 1972 *J. Phys. Soc. Japan* **33** 21
[8] Coey J M D, Viret M, Ranno L and Ounadjela K 1995 *Phys. Rev. Lett.* **75** 391
[9] Woodfield B F, Wilson M L and Byers J M 1997 *Phys. Rev. Lett.* **78** 3201
[10] Okuda T, Asamitsu A, Tomioka Y, Kimura T, Taguchi Y and Tokura Y 1998 *Phys. Rev. Lett.* **81** 3203
Okuda T, Tomioka Y, Asamitsu A and Tokura Y 2000 *Phys. Rev.* B **61** 8009
[11] Uhlenbruck S, Teipen R, Klingeler R, Bückner B, Friedt O, Hücker M, Kierspel H, Niemöller T, Pinsard L, Revcolevschi A and Gross R 1999 *Phys. Rev. Lett.* **82** 185
[12] Liu G-L, Zhou J-S and Goodenough J B 2001 *Phys. Rev.* B **64** 144414
[13] Syskakis E, Robens B and Naoumidis A 1993 *J. Physique Coll.* IV **3** C7 1429
[14] Pinsard L, Rodrígues-Carvajal J and Revcolevschi A 1997 *J. Alloys Compounds* **262/263** 152
[15] Kawano K, Kajimoto R, Kubota M and Yoshizawa H 1996 *Phys. Rev.* B **53** R14709
[16] Yamada Y, Hino O, Nohdo S and Kanao R 1996 *Phys. Rev. Lett.* **77** 904
[17] Kawano K, Kajimoto R, Yoshizawa H, Tomioka Y, Kuwahara H and Tokura Y 1997 *Phys. Rev. Lett.* **78** 4253
[18] Mills A J, Littlewood P B and Shraiman B I 1995 *Phys. Rev. Lett.* **74** 5144
[19] Röder H, Zang J and Bishop A R 1996 *Phys. Rev. Lett.* **76** 1356
[20] Mills A J 1996 *Phys. Rev.* B **53** 8434
[21] Mills A J, Shraiman Boris I and Mueller R 1996 *Phys. Rev. Lett.* **77** 175
[22] Ghivelder L, Castillo I A and Gusmao M A 1999 *Phys. Rev.* B **60** 12184
[23] Hamilton J J, Keatley E L, Ju H L, Raychaudhuri A K, Smolyaninova V N and Greene R L 1996 *Phys. Rev.* B **54** 14926
[24] Michalopoulou A, Papastaikoudis C and Syskakis E 2000 *Physica* B **284–288** 1412
[25] Ramirez A P, Schiffer P and Cheong S W 1996 *Phys. Rev. Lett.* **76** 3188
[26] Lees M R, Petrenko O A and Balakrishnan G 1999 *Phys. Rev.* B **59** 1298
[27] Paraskevopoulos M, Mayr F, Hartinger S, Pimenov A, Hemberger J, Lunkenheimer P, Loidl A, Mukhin A A, Ivanov V Yu and Balbashov A M 2000 *J. Magn. Magn. Mater.* **211** 118
[28] Coey J M D, Viret M and von Molnar S 1999 *Adv. Phys.* **48** 167
[29] Dabrowski B, Xiong X, Bukowski Z, Dybzinski R, Klamut P W, Siewenie J E, Chmaissem O, Shaffer J and Kimball C W 1999 *Phys. Rev.* B **60** 7006
[30] Kaveh M and Wiser N 1984 *Adv. Phys.* **33** 257
[31] Rice M J 1968 *Phys. Rev. Lett.* **20** 1439
[32] Kadowaki K and Woods S B 1986 *Solid State Commun.* **58** 507
[33] Dugdale J S 1976 *The Electrical Properties of Metals and Alloys* (Edward Arnold) p 240
[34] Kasuya T 1959 *Prog. Theor. Phys.* **22** 227
[35] Minnari I 1959 *Prog. Theor. Phys.* **22** 325
[36] Wang X and Zhang X-G 1999 *Phys. Rev. Lett.* **82** 4276
[37] Furukawa N 2000 *J. Phys. Soc. Japan* **69** 1954
[38] Michalopoulou A, Syskakis E and Papastaikoudis C 2001 *J. Phys.: Condens. Matter* **13** 11615
[39] Akimoto T, Moritomo Y, Nakamura A and Furukawa N 2000 *Phys. Rev. Lett.* **85** 3914
[40] Calderón M J and Brey L 2001 *Phys. Rev.* B **64** 140403
[41] Maebashi H and Fukuyama H 1998 *J. Phys. Soc. Japan* **67** 560
[42] Okuda T, Asamitsu A, Tomioka Y, Kimura T, Taguchi Y and Tokura Y 1998 *Phys. Rev. Lett.* **81** 3203
[43] Maebashi H 2003 private communication
[44] Mignot J-M, Ponchet A, Haen P, Lapierre F and Flouquet J 1989 *Phys. Rev.* B **40** 10917